

Perpendicular-electric-field dependence of exciton binding energy studied by continuous-wave photoluminescence

Kejian Luo, Houzhi Zheng, Shijie Xu, Xiaoping Yang, Penghua Zhang, Wei Zhang, and Chengfang Li

National Laboratory for Superlattices and Microstructures, Institute of Semiconductors, Chinese Academy of Sciences, Beijing 100083, People's Republic of China

(Received 30 November 1995)

The reduction of exciton binding energy induced by a perpendicular electric field in a stepped quantum well is studied. From continuous-wave photoluminescence spectra at 77 K we have observed an obvious blueshift of the exciton peak due to a spatially direct-to-indirect transition of excitons. A simple method is used to calculate the exciton binding energy while the inhomogeneous broadening is taken into account in a simple manner. The calculated result reproduces remarkably well the experimental observation. [S0163-1829(96)06023-7]

I. INTRODUCTION

It is well known that the exciton effect plays an important role in the optical properties of quantum-well (QW) structures. There has been a considerable amount of experimental and theoretical work on the exciton effect.¹⁻³ Particular attention has been paid to the effect on the exciton state of an electric field applied perpendicularly to the QW's interface. As recalled from theory, the exciton binding energy is expected to decrease under a perpendicular field, causing a blueshift of the exciton peak in the photoluminescence (PL) spectrum. However, the experimental investigation of this effect has been scarcely reported so far. This is because at the same time there exists another effect, the quantum confined Stark effect (QCSE), which leads to a redshift of the exciton peak with applied electric field. In conventional QW, the QCSE is the dominant effect. Therefore only a redshift has been well recorded in the PL spectra of QW structures over the years.³⁻⁵ In GaAs-AlAs superlattices, an indirect-direct anticrossing due to Γ - X mixing has been observed by Meynadier *et al.*, but the observed blueshift of the X line is mainly due to the existence of a voltage drop between adjacent layers and the change of the exciton binding energy is not discussed in their work.⁶

We specially designed a stepped QW to investigate how the exciton binding energy changes with perpendicular electric field. In this structure, the QCSE can be neglected in a certain bias range, so that the reduction of exciton binding energy dominates the behavior of the PL spectra. As a result, we directly observed a distinct blueshift stemming from the reduction of exciton binding energy from continuous-wave (cw) PL spectra, as reported in our previous paper.⁷ We experimentally demonstrated that the blueshift can be attributed to spatially direct-to-indirect transitions of excitons. In this paper, we present a simple but effective method to calculate the exciton binding energy of the stepped QW under various biases with the effect of the inhomogeneous broadening taken into account in a simple manner. We also make a close comparison with the exciton binding energies derived from PL spectra. It turns out that the calculated results are in good agreement with the experiment, in support of our previous experimental work.

The paper is organized as follows. In Sec. II, we describe the details of the sample structure in use. Then in Sec. III the experimental variation of the cw PL peak position with bias is briefly reviewed, as reported in Ref. 7. In Sec. IV, we perform the calculation of the exciton binding energy and compare it with the experiment. Finally, the main conclusions are summarized in Sec. V.

II. EXPERIMENTAL DETAILS

The structures used in our experiments are multilayered *n-i-n* heterostructures grown by molecular-beam epitaxy (MBE). A 0.6- μm -thick, Si-doped ($1 \times 10^{17} \text{ cm}^{-3}$), *n*-type GaAs buffer layer is deposited on an *n*-type (100) GaAs substrate (Si doped to $2 \times 10^{18} \text{ cm}^{-3}$). Then a nominally undoped multilayer consisting of GaAs/AlAs/GaAs/AlAs/GaAs/Al_{0.2}Ga_{0.8}As/Al_{0.4}Ga_{0.6}As (the corresponding thicknesses are 1000 Å/30 Å/40 Å/20 Å/25 Å/160 Å/500 Å) is grown in sequence. A 500-Å-thick *n*-type GaAs layer of $1 \times 10^{17} \text{ cm}^{-3}$ doping and a 200-Å-thick *n*-type GaAs cap layer of $4 \times 10^{18} \text{ cm}^{-3}$ doping are finally overgrown as the top contact layers. The energy-band profile of the structure under the flatband condition is sketched in Fig. 1(a).

The samples are processed into circle mesas of 2 mm diameter by conventional photolithography. Annular Ohmic contacts are fabricated by evaporating and subsequently alloying Au/Ge/Ni metals on the tops of the mesas. PL experiments are carried out at both 300 and 77 K. For the latter, the samples are held in a liquid-nitrogen cryostat. The photoexcitation is usually provided by the 4880 Å line of an Ar⁺-ion laser, and sometimes by the 7300 Å line of a Ti:sapphire laser in the case where a selective excitation is required. The excitation power density is kept at the level of 0.5 W/cm².

III. RESULTS OF EXPERIMENTS

As seen in Fig. 1(a), the structure is composed of one stepped QW on the left and one conventional QW on the right. They are separated by a 20-Å-thick AlAs barrier. The total width of the stepped QW is 185 Å with a deep portion of 25 Å. The conventional QW is 40 Å wide, used as the reference for comparison. We first perform a PL experiment under zero bias. Figure 2 shows the PL spectra excited by the

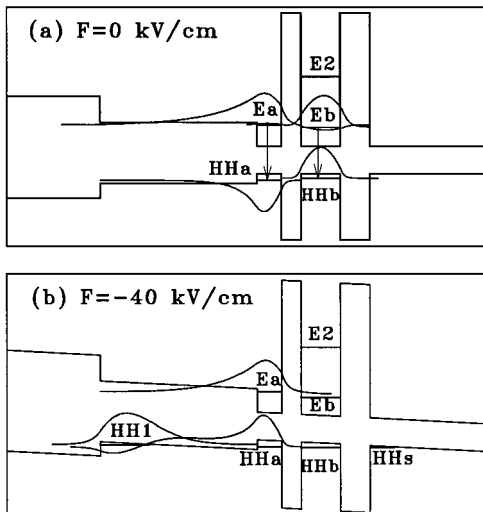


FIG. 1. Schematic band diagram of the structure and the wave functions of E_a , E_b , HH_a , and HH_b states (a) at $F=0$ kV/cm and (b) at $F=-40$ kV/cm.

4880 Å laser line, measured at 77 K (solid line) and 300 K (dashed line). Two peaks, A and B, are observed at both 77 and 300 K, with their photon energies labeled by E_{aa} and E_{bb} , respectively. From Fig. 1(a), it is rather intuitive to assign peak A to the transition from E_a to HH_a and peak B to the transition from E_b to HH_b . Here, E_a and HH_a denote the ground electron and hole states in the deep portion of the stepped QW; E_b and HH_b denote the ground electron and hole states in the conventional QW. From the PL spectrum measured at 300 K one obtains that $E_{aa}=1.636$ eV and $E_{bb}=1.612$ eV. In order to verify the above assignment we have used a simple envelope wave function method⁸ to calculate the transition energies for $E_a \rightarrow HH_a$ and $E_b \rightarrow HH_b$ in the absence of the exciton effect. The parameters used in the

calculation are as follows: the band offsets are $\Delta E_c=390$ meV and $\Delta E_v=195$ meV for $Al_{0.4}Ga_{0.6}As/GaAs$; $\Delta E_c=187$ meV and $\Delta E_v=80$ meV for $Al_{0.2}Ga_{0.8}As/GaAs$; and $\Delta E_c=1.058$ eV and $\Delta E_v=530$ meV for $AlAs/GaAs$. The effective masses have Al mole fraction (x) dependences given by $m_{\Gamma}^*=0.067+0.063x$, $m_{HH}^*=0.38+0.32x$, and $m_{LH}^*=0.095+0.055x$. The results show that the calculated transition energy for $E_a \rightarrow HH_a$ is equal to 1.639 eV and that for $E_b \rightarrow HH_b$ is 1.614 eV, in good agreement with the values measured at 300 K. This is what one expected because the thermal dissociation of excitons at 300 K is going to greatly suppress the exciton effect. It should be pointed out that no ambiguity of our assignment should arise from the complexity of the valence band, because the energy separation between the peaks A and B (23 meV at 77 K, 24 meV at 300 K) is much less than that between the ground heavy- and light-hole levels (66.3 meV in the conventional QW, 38.3 meV in the stepped QW, according to the calculation).

To provide further evidence for our assignment, we also carried out selective excitation experiment at 77 K. The excitation wavelength was tuned to 7300 Å which amounts to a photon energy of 1.702 eV. In this case, the excitation energy is lower than E_{aa} (1.716 eV), but higher than E_{bb} (1.693 eV) at zero bias. As a result, only peak B is observable on the low-energy side. As shown in the inset of Fig. 2, peak A does not appear until the negative bias goes beyond -0.8 V. Here, by ‘‘negative’’ we refer to the top contact being negatively biased with respect to the substrate. When a negative bias is applied to the structure, electrons will be injected into the QW’s from the n^+ electrode. On the other hand, as seen in Fig. 1(b), HH_b shifts downward more rapidly than HH_a with negative bias (linear Stark effect). Eventually, they cross each other as the electric field reaches a value of $F=-40$ kV/cm (about $V \approx -0.7$ V). As long as HH_b is below HH_a , the photoexcited holes in HH_b will partially be transferred to the level HH_a in the stepped QW through a nonresonant tunneling process. Then these holes in HH_a will recombine *in situ* with the electrons injected from the top n^+ electrode by emitting photons. This gives rise to the reappearance of a weak peak A on the high-energy side when the bias is higher than -0.8 V. The above selective excitation experiment further indicates the correctness of our assignment.

We now turn to studying the bias dependences of E_{aa} and E_{bb} at 77 K systematically. Figure 3 plots the variation of E_{aa} and E_{bb} with the bias voltage. The remarkable feature of it is that E_{aa} displays an abrupt blueshift of about 6 meV in the bias range from -0.5 to -1.0 V, in contrast to the expected redshift. Let us first claim tentatively that this anomalous blueshift can be attributed to the reduction of exciton binding energy in the stepped QW. By applying negative bias, a transition from spatially direct to spatially indirect excitons may easily occur for the following reason. Under negative biases, as seen in Fig. 1(b), the electron wave function of E_a becomes more localized in the deep portion of the stepped QW. Meanwhile, the hole wave function of HH_a is going to extend from the deep portion to the whole stepped QW. As a result, the Coulomb interaction inside the exciton will be significantly weakened because of the enlarged spatial separation between the electron and hole. This will certainly result in a noticeable reduction of exciton binding en-

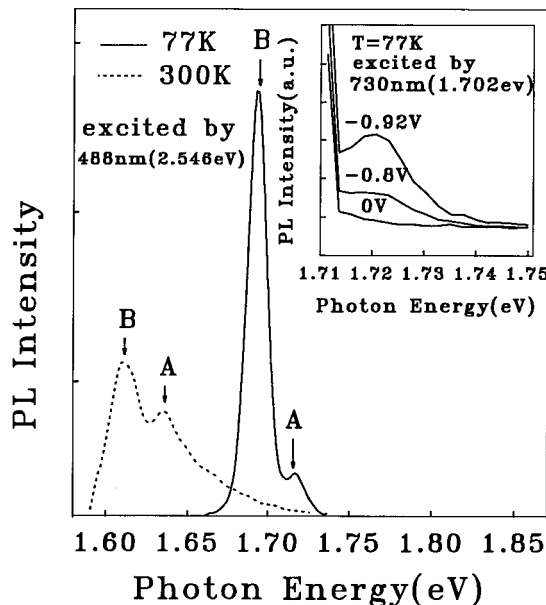


FIG. 2. PL spectra at 77 K (solid line) and 300 K (dashed line) under zero bias. The inset shows PL spectra excited by the 7300 Å laser line at 77 K under biases of 0, -0.8 , and -0.92 V.

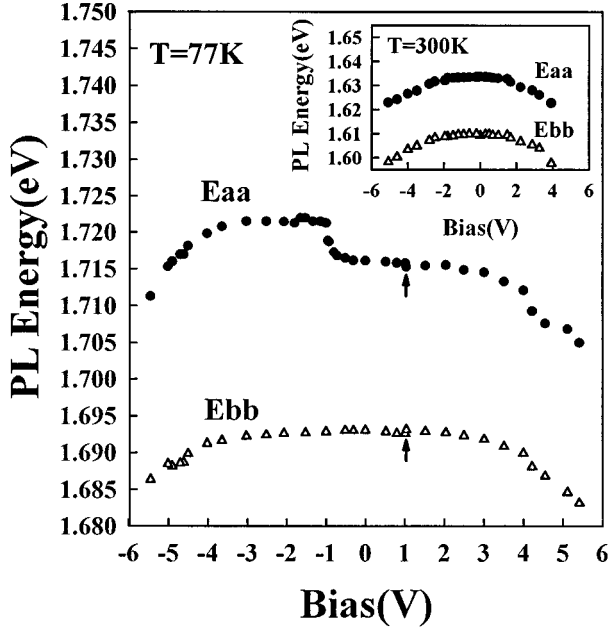


FIG. 3. Variation of E_{aa} (●) and E_{bb} (△) with bias at 77 K. The inset shows the bias dependence of E_{aa} and E_{bb} at 300 K.

ergy. At the same time, the Stark shift of E_{aa} is rather small (not more than 1 meV according to our calculations) due to the very narrow width (25 Å) of the deep portion in the stepped QW. Accordingly, the observed blueshift of E_{aa} is obviously caused by the reduction in the exciton binding energy in the bias range from -0.5 to -1.0 V. However, the QCSE will eventually surpass the mentioned effect if the bias is continually increased, showing a redshift at large negative biases ($|V| > 4$ V). Under a positive bias the situation is quite different. At biases where the electron wave function starts to spill out of the deep portion of the stepped QW, the Stark shift of E_{aa} also becomes strongest at the same time, as demonstrated by our envelope function calculation. The two opposite effects likely cancel each other, leading to a rather small spectroscopic shift in the bias range from 0 to 3 V.

Previously, in coupled QW's, one also observed an abrupt change in the PL peak position, stemming from the level repulsion.^{9,10} However, the observed blueshift of E_{aa} in the present case cannot be ascribed to the crossing of electron levels in the conduction band. On one hand, E_b is already below E_a under zero bias and will continuously descend away from E_a with increasing negative bias. On the other hand, the field used in our experiments is not high enough to bring E_2 in resonance with E_a since the energy separation between E_b and E_2 is as high as 400 meV. Here E_2 is the first excited state in the conventional QW [see Fig. 1(a)]. Therefore, E_a cannot cross both E_b and E_2 under negative bias. For the crossing of hole levels in the valence band, the resultant energy splitting is expected to be no more than 1 meV.¹¹ This small level repulsion cannot account for the observed large blueshift (6 meV) under negative bias. However, under positive bias we have seen a very small redshift in E_{aa} and a very small blueshift in E_{bb} as the bias passes through +1 V, as indicated by two arrows in Fig. 3. This is a typical feature of repulsion. From our calculation, the resonant coupling between E_a and E_b indeed takes place at the corresponding bias, which gives rise to the observed level

repulsion. The calculated energy splitting for the electron levels (~ 4 meV) is much larger than the measured value (0.6 meV). Such a discrepancy presumably arises from the weakened coupling between the two wells because of interface defects, impurity scattering, etc.¹²

Furthermore, we have measured the same bias dependences of E_{aa} and E_{bb} at 300 K. The result is shown in the inset of Fig. 3. No blueshift is observed. As mentioned previously, the thermal ionization of excitons will become increasingly important. A PL signal featuring the recombination of free electrons and holes will dominate over exciton-type PL as kT becomes comparable with the exciton binding energy. Especially in the present case, the closeness of the electron level E_a to the top of the broad part of the stepped QW makes the carriers spill out of the deep portion of the stepped QW more easily at elevated temperatures. That further facilitates the dissociation of the excitons at 300 K, although the excitonic feature of PL spectra can be observable at 300 K in high-quality MBE-grown multiple quantum wells as demonstrated by many authors.¹³ For the mentioned reason, the blueshift of E_{aa} shown in Fig. 3 should most probably disappear at 300 K, as seen in the inset of Fig. 3.

For comparison, we also measure the bias dependences of E_{bb} at 77 and 300 K (as seen in Fig. 3). It shows that the variation of E_{bb} is dominated by the QCSE, a typical phenomenon in conventional QW's.

In Sec. IV, we will calculate the exciton binding energies at various biases and reproduce the main features of our observation at 77 K.

IV. CALCULATION OF EXCITON BINDING ENERGY

To compare the measured results with theories, in this section, we adopt a simple method developed by Leavitt and Little,¹⁴ and calculate the bias dependence of the exciton binding energy for the stepped QW in use. Generally speaking, the various methods for calculating the exciton binding energy basically fall into two kinds. One is the variational method, featuring a proper choice of a specific form for the excitonic wave function. Its disadvantage is that the appropriate form of the wave function cannot be made generic and must be altered if the structure is changed. The other method is to first integrate out the Z coordinate to obtain an equation describing the radial motion in the plane of the exciton envelope function. While the second method is universal in contrast to the first one, it suffers from several drawbacks. One usually encounters the difficulty of solving a relatively complicated eigenvalue problem in order to obtain each binding energy. Moreover, in the second approach, the exciton envelope function does not contain any dependence on the Z axis other than that contained in the subband envelope functions. As a result, the correlated motion of the electron and hole along the Z direction is neglected, and the partially three-dimensional nature of the exciton in wider QW's (e.g., in the wider portion of our stepped QW) is not properly characterized. Leavitt and Little employed a similar method to that used in the Born-Oppenheimer separation of electronic and nuclear coordinates,¹⁵ and separated the radial and perpendicular motions of the exciton. The former is quasi-two-dimensional, but dependent on the spatial separation between the electron and hole along the Z direction in a para-

metric manner. The latter includes the correlated nature of the electron and hole within the exciton. This method could be applicable to a variety of complex quantum-confined semiconductor structures for which more rigorous approaches require extensive numerical calculations. Therefore Leavitt and Little's method is specially suitable for our present purpose. Following Leavitt and Little, we shall adopt the assumptions that both band nonparabolicity and valence-band mixing are neglected, and each exciton is constructed from a specific pair of electron and hole subbands. The formula of the exciton binding energy may directly be written as

$$E_{ij}^B = \int_{-\infty}^{\infty} dZ_e dZ_h E_0 |f_i^{(e)}(Z_e)|^2 |f_j^{(h)}(Z_h)|^2 E_1^{(2D)}(Z_e - Z_h). \quad (1)$$

Here, the Z axis is defined as perpendicular to the structure's interfaces. Z_e and Z_h are the electron and hole positions in the Z direction. E_{ij}^B denotes the binding energy of the exciton associated with the i th electron subband and the j th hole subband. $f_i^{(e)}(Z_e)$ and $f_j^{(h)}(Z_h)$ are the corresponding electron and hole envelope wave functions, respectively. $-E_1^{(2D)}(Z)$ ($Z = Z_e - Z_h$) is the eigenenergy of the exciton's ground state ($n=1$), and can be obtained by solving the following radial Schrödinger equation:

$$\begin{aligned} -\frac{\hbar^2}{2\mu_{\parallel}} \frac{1}{\rho} \frac{d}{d\rho} \left[\rho \frac{dg_1(\rho; Z)}{d\rho} \right] - \frac{e^2}{\varepsilon(\rho^2 + Z^2)} g_1(\rho; Z) \\ = -E_1^{(2D)}(Z) g_1(\rho; Z). \end{aligned} \quad (2)$$

Clearly, both $E_1^{(2D)}(Z)$ and $g_1(\rho; Z)$, the exciton's envelope wave function, depend parametrically on the Z coordinate through the Coulomb potential. Equation (1) represents the binding energy for a two-dimensional exciton, with the electron and hole located, respectively, at Z_e and Z_h , weight averaged by the probability of finding an electron at Z_e and a hole at Z_h .

Leavitt and Little solved the above eigenequation, Eq. (2) by using a 15-parameter variational wave function, and fitted the width dependence of $E_1^{(2D)}(Z)$ by the following polynomial:

$$w(v) = \frac{4 + c_1 v + c_2 v^2}{1 + d_1 v + d_2 v^2 + d_3 v^3}. \quad (3)$$

Here $w(v) = E_1^{(2D)}(Z)/E_0$ and $v = Z/a_0$, expressed in dimensionless forms. E_0 and a_0 , the effective Rydberg energy and Bohr radius, are given by $E_0 = \mu_{\parallel} e^4 / 2\varepsilon^2 \hbar^2$ and $a_0 = \varepsilon \hbar^2 / \mu_{\parallel} e^2$, $\mu_{\parallel} = m_e m_{h_{\parallel}} / (m_e + m_{h_{\parallel}})$, where m_e and $m_{h_{\parallel}}$ are the effective masses in the conduction band and valence band for the motion in the plane. The parameters in Eq. (3) are obtained to be

$$\begin{aligned} c_1 = 12.97, \quad c_2 = 0.7180, \quad d_1 = 9.65, \\ d_2 = 9.24, \quad d_3 = 0.3706. \end{aligned} \quad (4)$$

In what follows, we shall focus our interest on calculating the binding energy of the $n=1$ heavy-hole exciton in the deep portion of the stepped QW using Eqs. (1), (3), and (4). The parameters used in the calculation are $\varepsilon = 13.2$,

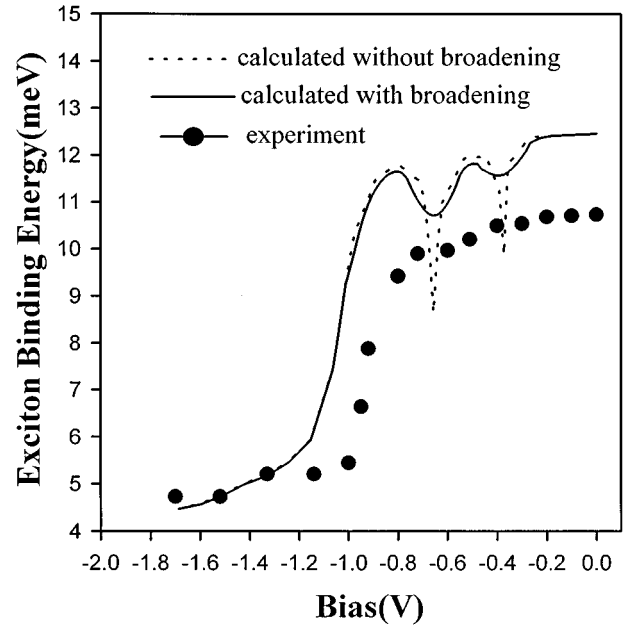


FIG. 4. Calculated and experimental bias dependence of exciton binding energy in the stepped QW. The dotted line is the result calculated without any broadening. The solid line is that calculated with inhomogeneous broadening. The solid circles are the experimental results obtained from Eq. (7).

$m_e = 0.067 + 0.063x$, and $m_{h_{\parallel}} = 0.217 + 0.106x$, where x is the Al mole fraction. Other parameters needed for calculating $f_i^{(e)}(Z_e)$ and $f_j^{(h)}(Z_h)$ are listed in Sec. III. In order to compare with experiment, we convert the electric-field values into bias values by assuming that the electric field is linearly applied to the undoped region. The dashed line in Fig. 4 plots the results calculated from Eqs. (1), (3), and (4). It shows that the exciton binding energy decreases sharply from -0.7 to -1.2 V (the corresponding field range is from -40 to -70 kV/cm). Two dips appear at about -0.4 and -0.65 V corresponding to the hole level HH_a in resonance with HH_1 and HH_b , respectively [as seen in Fig. 1(b)]. However, no such dips are observed in the experiment. In reality, the level broadening, either inhomogeneous or homogeneous, will smear out such a sharp resonant feature. Accordingly, the inhomogeneous broadening should be included in the calculation of the binding energies. The inhomogeneous broadening is usually caused by well-width fluctuation, alloy disorder, carrier scattering, etc. At 77 K, peak A has a Gaussian line shape with the full width at half maximum (FWHM) of 14 meV at zero bias. For simplicity, we assume the broadening is only from a Gauss-like well-width fluctuation in the deep portion of the stepped QW, as given by

$$\varphi(W_i) = \frac{1}{\sqrt{\pi}} \frac{2\sqrt{\ln 2}}{\Gamma} \exp\left\{-\left[\frac{|W_i - W_0|}{\Gamma} 2\sqrt{\ln 2}\right]^2\right\}, \quad (5)$$

where $\varphi(W_i)$ is the probability for the exciton to reside at the well width of W_i , W_0 is the nominal well width (25 Å) given for the sample growth in our experiments, and Γ is the FWHM of $\varphi(W_i)$, which is calculated to be 3 Å, corresponding to the FWHM (14 meV) of peak A. We first calculate exciton binding energies at different well widths using Eqs.

(1), (3), and (4). Then we make a weighted average of the binding energy by using a Gauss law:

$$\overline{E^B} = \int_{-\infty}^{\infty} E^B(W_i) \varphi(W_i) dW_i, \quad (6)$$

where $E^B(W_i)$ denotes the exciton binding energy calculated at the well width of W_i .

The solid line of Fig. 4 shows the results obtained from Eq. (6). We can see that the two dips tend to be washed away, but the overall shape does not change. It is apparent that our calculation reproduces the main features of our observation, even when considering the inhomogeneous broadening in such a simple manner.

We also derive the exciton binding energies directly from the PL spectra. As discussed in Sec. III, the Stark shift of E_{aa} is not more than 1 meV in the field range where the blueshift occurs. In Fig. 3, a redshift of E_{aa} is not observed until -1.8 V. In the bias range from 0 to -1.8 V, the shift of E_{aa} is mainly due to the reduction of the exciton binding energy. The blueshift of E_{aa} reaches its maximum at -1.7 V. When the bias is beyond -1.7 V, we assume that the exciton binding energy is close to the exciton binding energy of bulk GaAs (4.2 meV). Then we can estimate the exciton binding energy as follows:

$$E^B(V_b) = E_{aa}(-1.7 \text{ V}) - E_{aa}(V_b) + 4.2 \text{ meV}, \quad (7)$$

where $E_{aa}(-1.7 \text{ V})$ stands for the E_{aa} value at -1.7 V, and $E_{aa}(V_b)$ is the E_{aa} value at one particular bias V_b in the range from 0 to -1.7 V. The solid dots in Fig. 4 show the results derived from Eq. (7). It is obvious that the calculated results are in good agreement with the experimental values.

V. SUMMARY

We have observed the spatially direct-to-indirect transition of excitons by studying the spectroscopic shift of the PL peak in a stepped QW with increasing perpendicular electric field. The distinct blueshift of the PL peak at 77 K and its absence at 300 K provide convincing evidence for the reduction of the exciton binding energy due to such a transition. To justify our statement, we present a simple method to calculate the exciton binding energy, while the inhomogeneous broadening is included in a simple manner. The calculated results are in good agreement with the experimental ones. Our work may give a convenient way to measure the exciton binding energy directly from conventional PL spectra.

ACKNOWLEDGMENTS

The authors would like to thank Wei Liu for technical assistance. This work is supported by the State Science and Technology Commission and Chinese National Natural Science Foundation.

-
- ¹Y. Tokuda, K. Kanamoto, and N. Tsukada, *Appl. Phys. Lett.* **56**, 166 (1990), and references therein.
²D. A. B. Miller, J. S. Weiner, and D. S. Chemla, *IEEE J. Quantum Electron* **QE-22**, 1816 (1986).
³D. A. B. Miller, D. S. Chemla, T. C. Damen, A. C. Gossard, W. Wiegmann, T. H. Wood, and C. A. Burrus, *Phys. Rev. B* **32**, 1043 (1985).
⁴R. T. Collins, K. V. Klitzing, and K. Ploog, *Phys. Rev. B* **33**, 4378 (1986).
⁵S. Tarucha and K. Ploog, *Phys. Rev. B* **38**, 4198 (1988).
⁶M.-H. Meynadier, R. E. Nahory, J. M. Worlock, M. C. Tamargo, J. L. de Miguel, and M. D. Sturge, *Phys. Rev. Lett.* **60**, 1338 (1988).
⁷K. J. Luo, H. Z. Zeng, S. J. Xu, P. H. Zhang, W. Zhang, and X. P. Yang, *Appl. Phys. Lett.* **67**, 2642 (1995).

- ⁸C. Weisbuch and B. Vinter, *Quantum Semiconductor Structures* (Academic, San Diego, 1991), Chap. II.
⁹Y. Tokuda, K. Kanamoto, Y. Abe, and N. Tsukada, *Phys. Rev. B* **41**, 10 280 (1990).
¹⁰Y. Tokuda, K. Kanamoto, N. Tsukada, and T. Nakayama, *Appl. Phys. Lett.* **54**, 1232 (1989).
¹¹L. Vina, R. T. Collins, E. E. Mendez, and W. I. Wang, *Phys. Rev. Lett.* **58**, 832 (1987).
¹²F. Capasso, K. Mohammed, and A. Y. Cho, *IEEE J. Quantum Electron* **QE-22**, 1853 (1986).
¹³P. Dawson, G. Duggan, H. I. Ralph, and K. Woodbridge, *Phys. Rev. B* **28**, 7381 (1983).
¹⁴R. P. Leavitt and J. W. Little, *Phys. Rev. B* **42**, 11 774 (1990).
¹⁵A. Messiah, *Quantum Mechanics* (Wiley, New York, 1963), Vol. II, pp. 781–793.